SIZE-DEPENDENT EFFECTS

Sol–gel preparation and characterization of perovskite lanthanum lithium titanate

Ionela Carazeanu Popovici · Elisabeta Chirila ·
Viorica Popescu · Victor Ciupina · Gabriel Prodan

Abstract Lanthanum lithium titanate, belonging to the solid solution $La_{0.66}Li_{0.33}TiO_3$, was prepared by sol–gel method from $LiNO_3$, $La(NO_3)_3 \cdot 6H_2O$ and $Ti(OC_4H_9)_4$ in ideal cation stoichiometry for $La_{0.66}Li_{0.33}TiO_3$. The synthesized product was characterized by X-ray powder diffractometry (XRD) and thermal analyses (DTA-TG). Electron microscopy investigations (SEM and TEM) was used to evaluate the morphology of synthesized $La_{0.66}Li_{0.33}TiO_3$.

The bulk quantities of nano-sized particles of layered $La_{0.66}Li_{0.33}TiO_3$ have been obtained at 1,000°C using the modified sol–gel method. The mean diameter of $La_{0.66}Li_{0.33}TiO_3$ nano-crystals was about 123 nm.

Introduction

Ionic conducting solid materials have received considerable attention in the last few years due to their potential utility in several solid state devices: electrochemical sensors, secondary (rechargeable) batteries, electrochromic displays etc.

The studies of solid electrolytes with lithium ionic conductivity have been of much interest because of potential applications in battery systems. Oxides like

I. Carazeanu Popovici (✉) · E. Chirila · V. Popescu
Chemistry Department, Ovidius University, 124 Mamaia,
Constantza, Romania
e-mail: icarazeanu@univ-ovidius.ro

V. Ciupina · G. Prodan
Electron Microscopy Laboratory, Ovidius University,
Constantza, Romania

$La_{1-x}Li_xTiO_3$ present a perovskite—type structure (ABO_3) with cation deficiency at the A-sites. It has been shown that this deficiency is favorable for high ionic mobility of monovalent cations through the bottleneck formed by four adjacent BO_6 octahedra. Since the A- and B- sites in this structure can tolerate different ions with different valence states, several studies have been reported on the influence on the ionic conductivity of the A-site substitution in $Ln_{0.5}Li_{0.5}TiO_3$ (Ln = La, Pr, Nd, Sm) and B-site substitution in $Ln_{1/3}Li_xNb_{1-x}Ti_xO_3$ (Ln = La, Nd). Moreover and since these compounds present some vacancies in their structure, intercalation of lithium ions can be considered [1–9].

The $La_{1-x}Li_xTiO_3$ powders have been previously synthesized by solid-state reactive firing of reagent grade starting materials like La_2O_3 and TiO_2 and Li_2CO_3 mixed in appropriate amounts. The formation of $La_{1-x}Li_xTiO_3$ phase necessitated to repeat the thermal treatment at 800°C for 4 h, 1,150°C for 28 h and 1,250°C for 12 h; after that the thermal treatment powders were sintered at 1,350°C for 6 h [10, 11]. Research works in this area have focused the attention on new synthesis route for low-temperature crystallized oxides, which showed some promise in improving the cycle life of rechargeable lithium batteries. Several wet-chemical methods have been used to obtain solid solution with better homogeneity and control of stoichiometry by several other researchers. Among these, coprecipitation and sol–gel are the most widely investigated for ceramic powder preparations. The powders obtained from the coprecipitation technique are highly agglomerated in nature and further ball milling is necessary to obtain fine powders with small particle size. The success of sol–gel process in the synthesis of ceramic powders is due, in particular, to the possibility

of working at low temperature and attaining good homogeneity in the solution phase. This method for the synthesis of inorganic materials has a number of advantages over more conventional synthetic procedures. For examples, high purity materials can be obtained by mixing precursor solutions [12–17].

In this paper we present the results obtained on the powder X-ray diffraction (XRD), thermal analysis (TG-DTA) and electron microscopy (SEM and TEM) studies of lanthanum lithium titanate $La_{0.66}Li_{0.33}TiO_3$ synthesized by the modified sol–gel method.

Experimental

Figure 1 shows a flowchart of the synthesis procedure for lanthanum lithium titanate powders by the sol–gel method. Lanthanum lithium titanate powders was synthesized by the modified sol–gel method from $LiNO_3$, $La(NO_3)_3 \cdot 6H_2O$ and titanium butoxide $Ti(OC_4H_9)_4$ (Merck reagents with purities > 99%) in ideal cation stoichiometry for $La_{0.66}Li_{0.33}TiO_3$. The method is based on condensation polymerization

between ethylene glycol ($HOCH_2CH_2OH$) and citric acid $(HOH)(CO_2H)(CH_2CO_2H)_2$ in presence of soluble metal–citrate complexes. The precursor samples were heat-treated between 600 and 1,100 °C during 2 h. The molar ratio of the metals was determined by inductive coupled plasma—mass spectrometry using an ICP-MS Agilent 7500a device [18].

The synthesized product was characterized by X-ray powder diffractometry (XRD) and thermal analyses (DTA-TG). Electron microscopy experiments (SEM and HRTEM) was used to evaluate the morphology of synthesized $La_{0.66}Li_{0.33}TiO_3$.

Simultaneous differential thermal analysis (DTA) and thermogravimetric analysis (TGA) experiments of the polymerized complex gel precursor of $La_{0.66}Li_{0.33}TiO_3$ were made using a Shimadzu DTG-TA-51H device. The synthesized powders were characterized by XRD. X-ray diffraction experiments were performed on a Shimadzu 6,000 automatic diffractometer equipped with a graphite monochromator and CuK_α radiation ($\lambda = 1.5406$Å, the scanning region 2θ was equal to 20–80°). Microstructural investigation of synthesized powders was performed using scanning electron

Fig. 1 Synthetic procedure of $La_{0.66}Li_{0.33}TiO_3$ powder

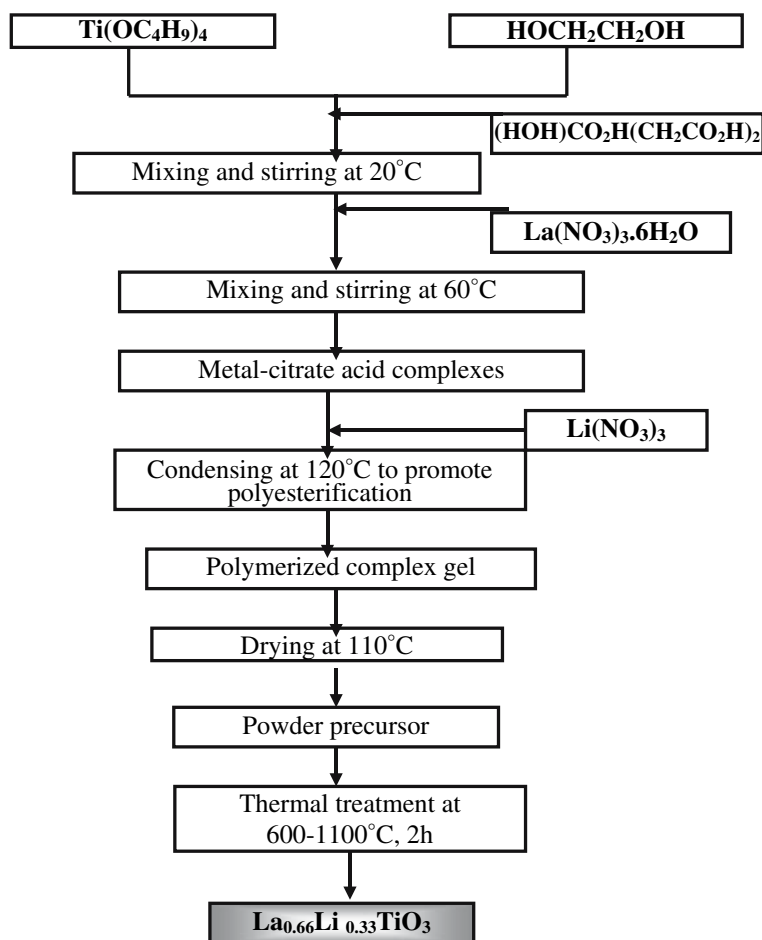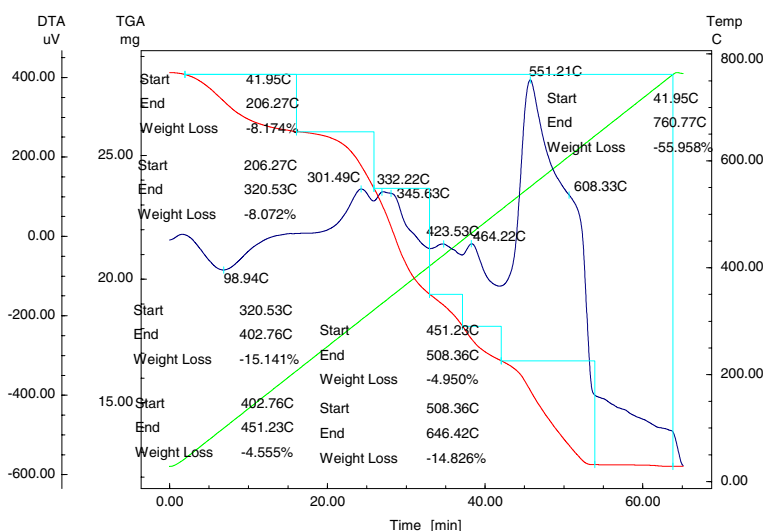**Fig. 2** DTA-TG curves of
$La_{0.66}Li_{0.33}TiO_3$ powder
precursor

microscopy (SEM) with Jeol JMS 5,800 L electron microscope. The samples were coated with gold and examined in the as-fired condition, i.e., without polishing. High-resolution transmission electron microscopy (HRTEM) was used to evaluate the purity and the phase composition of $La_{0.66}Li_{0.33}TiO_3$. The bright field—transmission electron microscopy (BF-TEM) investigations was made with Philips CM 120 ST microscope operating at 100 kV and magnification maxim 1,200,000×. The resolution obtained in our cases was about 2Å. Lattice plane images give information about crystal structure and selected area electron diffraction (SAED) images help us to identify the phase. Also the crystals size distribution was studied.

Results and discussions

ICP chemical analysis showed that the cations' molar ratio corresponds to the formula $La_{0.66}Li_{0.33}TiO_3$. We

have estimated the oxygen content by balancing the electroneutrality of the solid. Figure 2 shows the DTA-TG curves, which display the formation temperature of the $La_{0.66}Li_{0.33}TiO_3$ obtained by the modified sol–gel method. An endothermic peak appears on DTA curve at 99 °C corresponding to water adsorbed in the pores and exothermic peaks (301, 332, 345, 423, 464, 551 and 608 °C) corresponding to the combustion of the acid metal–citric complex. It appeared that the mix citric acid + ethylene glycol act as a complexing agent in the pyrolysis of the gel precursor, accelerating the decomposition of metal–citric acid complexes and the formation of $La_{0.66}Li_{0.33}TiO_3$ oxide.

The X-ray diffraction patterns of nanocrystalline $La_{0.66}Li_{0.33}TiO_3$ powders obtained by the modified sol–gel method was recorded. The X-ray patterns for the precursor and the samples treated below 750 °C

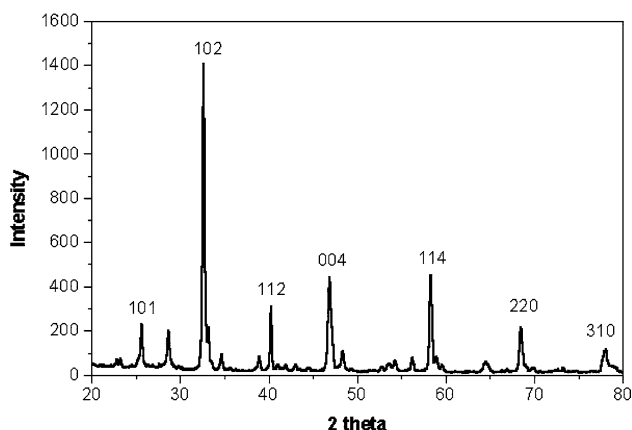**Fig. 3** XRD patterns of $La_{0.66}Li_{0.33}TiO_3$ powders obtained by the sol–gel method

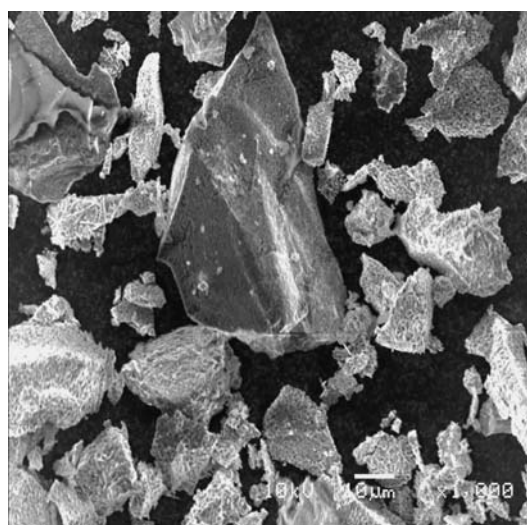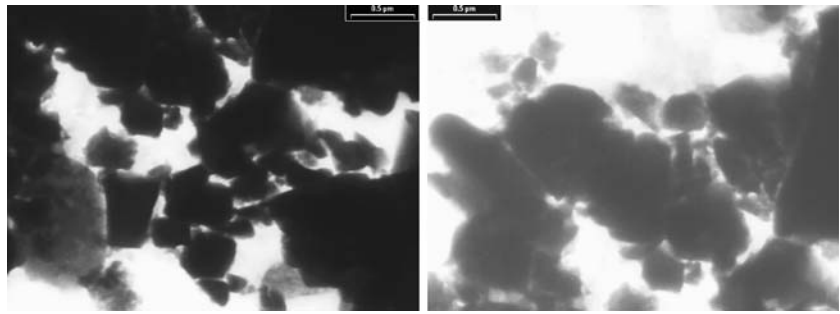**Fig. 4** SEM micrograph of $La_{0.66}Li_{0.33}TiO_3$ powders synthesized by thermal treatment at 1,000 °C for 2 h

Fig. 5 BF-TEM micrograph of $La_{0.66}Li_{0.33}TiO_3$ powders synthesized by thermal treatment at 1,000 °C for 2 h

were primarily those of amorphous solids, indicating that the precursor sample was not crystallized at low temperatures. The presence of both $La_{0.66}Li_{0.33}TiO_3$ and amorphous phases in obtained sample heat-treated at 800 °C was detected. All XRD reflections of the obtained sample heat-treated above 900 °C exhibited a single phase of $La_{0.66}Li_{0.33}TiO_3$. The most significant X-ray pattern indicates that the crystallization of the $La_{0.66}Li_{0.33}TiO_3$ phase is complete at 1,000 °C. Figure 3 shows the XRD pattern of synthesized $La_{0.66}Li_{0.33}TiO_3$ after thermal treatment for 2 h at 1,000 °C. The X-ray diffraction patterns were indexed in a tetragonal cell with $a = b = 3.87$Å and $c = 7.74$ Å.

Surface morphology and texture as well as particles size of the synthesized $La_{0.66}Li_{0.33}TiO_3$ were observed by SEM and TEM investigations. In the Fig. 4 are

presented the SEM imagines for of the synthesized $La_{0.66}Li_{0.33}TiO_3$ and in the Fig. 5 are presented the micrograph obtained by bright field—transmission electron microscopy investigations (BF-TEM).

The TEM samples are deposited on 300 mesh grid formvar coated from 10 wt% nanoparticles in ethanol. BF-TEM reveal a large agglomerate of nanoparticles with dimensions below 1 μm. The particle diameter is evaluated by mean value of the distances between pairs of parallel tangents to the projected outline of the particle (Feret's diameter) and mean diameter is calculated assuming a lognormal distribution of experimental data.

Diameters distribution and fitting curve assume a lognormal distribution for diameter dispersion (Fig. 6). The lognormal function used for fit the experimental curves is given by (1):

$$y = Ae^{-\frac{\ln^2(x/x_C)}{2w^2}} \tag{1}$$

where A is an arbitrary constant related to particle number, x_c represent the distribution maximum and w is strong correlated with particle diameter dispersion.
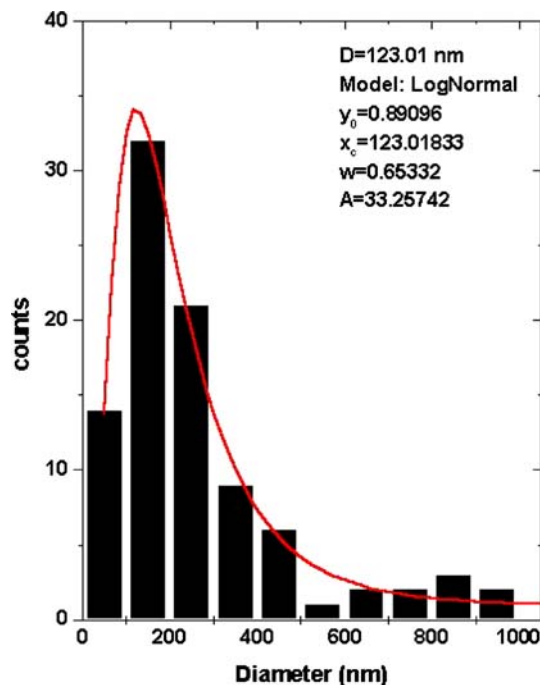

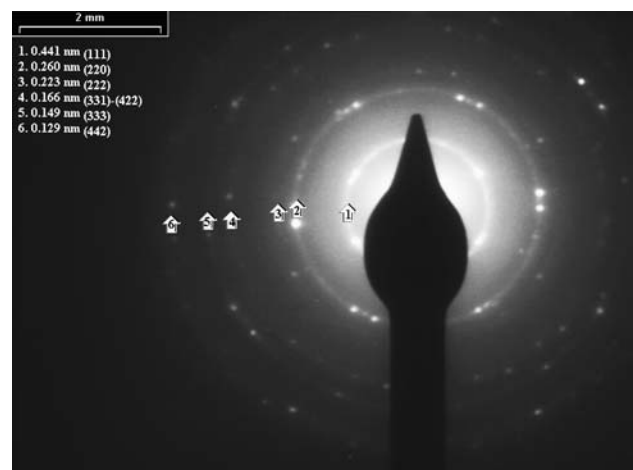**Fig. 6** Diameters distribution and fitting curve assuming a lognormal distribution
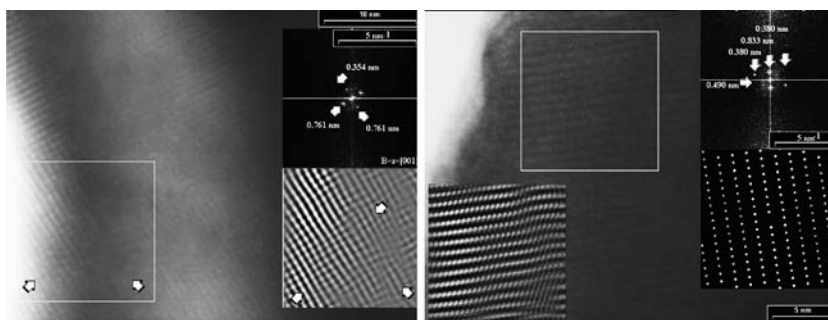

Fig. 7 SAED image of $La_{0.66}Li_{0.33}TiO_3$ powder

Fig. 8 HRTEM image of
tethragonal single crystal of
$La_{0.66}Li_{0.33}TiO_3$ orientated
along [001] axis

Using Scherer relation we can estimate the mean diameter. The relation (2):

$$D = \frac{57.3 \cdot k \cdot \lambda}{\beta \cdot \cos\theta} \qquad (2)$$

implies the use of k shape factor of particles, β half intensity width and θ Bragg angle for selected ring.

The HRTEM investigation of obtained particles shows that the single crystal structure of $La_{0.66}Li_{0.33}TiO_3$ is tetragonal with $a = 0.387$ nm and $c = 0.775$ nm.

The phases that are present in $La_{0.66}Li_{0.33}TiO_3$ powder are identified with selected area electron diffraction (SAED) as shown in Fig. 7. This figure shows the SAED image of $La_{0.66}Li_{0.33}TiO_3$ powder that shows presence of large crystal (bright spot on diffraction rings). In the Fig. 8 are presented SAED patterns of tetragonal single crystal orientated along [001] axis. Rigth insert represent FFT amplitude of selected area from image and down filtered image using a blob filter that keep only spot from FFT image.

Conclusions

The $La_{0.66}Li_{0.33}TiO_3$ powders in the sample prepared by sol–gel method are formed at a lower temperature than the temperature needed to obtain this solid solution by the conventional solid-state reaction. The early formation of the $La_{0.66}Li_{0.33}TiO_3$ starts at 700 °C; the sol–gel method appeared to be more suitable due to the mixing of elements at molecular level during the synthesis. Crystallization of the $La_{0.66}Li_{0.33}TiO_3$ phase began at temperature below 800 °C and becomes complete at 1,000 °C.

The optimum heating temperature for synthesized $La_{0.66}Li_{0.33}TiO_3$ by modified sol–gel method is 1,000 °C. The $La_{0.66}Li_{0.33}TiO_3$ nano-crystals with mean diameter of about 123 nm were obtained by modified sol–gel method.

References

1. Joo Lee H, Min Park H, Koo Cho Y (2003) J Am Ceram Soc 86:1395
2. Keshimiri M, Troczynski T (2003) J Non-Crystalline Solids 324:289
3. Zhang W, Liu W, Li B (2002) J Am Ceram Soc 85:1770
4. Emery J, Buzare JY, Bohnke O, Fourquet JL (1997) Solid State Ionics 99:41
5. Inaguma Y, Liquan C, Itoh M, Nakamura T, Uchida T, Ikuta H, Wakihara M (1993) Solid State Com 86:689
6. Bohnke O, Bohnke C, Fourquet JL (1996) Solid State Ionics 91:21
7. Crosnier-Lopez MP, Duroy H, Fourquet JL (1999) Mat Res Bulletin 34:179
8. Borisevich AY, Davies PK (2002) J Am Ceram Soc 85:2487
9. Thangadurai V, Heiko H, Weppner WJF (2003) J Am Ceram Soc 86:437
10. Varez A, Garcia-Alvarado F, Moran E, Alario-Franco MA (1995) J Solid State Chem 118:78
11. Inaguma Y, Katsumata T, Itoh M, Morii Y (2002) J Solid State Chem 166:67
12. Tarascon JM, Guyomard D (1993) Electrochimica Acta 38:1221
13. Ovenston A, Qin D, Walls JR (1995) J Mater Sci 30:2496
14. Zhou Y, Li H (2002) J Solid State Chem 165:247
15. Ciupina V, Carazeanu I, Prodan G, Guguta C (2004) Microchim Acta 147:151
16. Ciupina V, Carazeanu I, Prodan G, Vasile E (2003) Balkan Phys Lett 11:128
17. Ciupina V, Carazeanu I, Prodan G (2004) J Optoelect Adv Mat 6:1317
18. Petisleam T, Chirila E, Caradima Z (2005) Rev Chim (Bucharest) 12:1222